Eur Biophys J (2003) 32: 342–354
DOI 10.1007/s00249-003-0282-2

ARTICLE

Damien Cuvelier · Olivier Rossier
Patricia Bassereau · Pierre Nassoy

Micropatterned "adherent/repellent" glass surfaces for studying the spreading kinetics of individual red blood cells onto protein-decorated substrates

Received: 30 August 2002 / Revised: 11 December 2002/Accepted: 19 December 2002 / Published online: 19 February 2003

Abstract We report in this paper two simple and effective methods to decorate glass surfaces that enable protein micropatterning and subsequent spatially controlled adhesion of cells. The first method combines simultaneously the potentialities of two existing techniques, namely microcontact printing (μCP) and microfluidic networks (μFN) to achieve dual protein patterning in a single step. The second method is mainly based on the well-known property of poly(ethylene glycol) (PEG) to resist against protein adsorption. Both approaches were used to produce heterogeneous surfaces on which micron-size or submicronic streptavidin-coated lines alternate with cell-repellent areas. We first describe the implementation of the two methods and discuss the main pitfalls to avoid. Then, using these templates, we have monitored the kinetics of attachment of individual biotinylated (i.e. "attractant" towards streptavidin) red blood cells by directly measuring the propagation velocity of the adhesion front. Depending on the surface density of biotin, we found two distinct regimes, in agreement with existing theoretical models.

Keywords Cell attachment kinetics · Microfluidic networks · Protein patterning · Red blood cells · Reflection interference contrast microscopy

Abbreviations μCP: microcontact printing · μFN: microfluidic networks · BSA: bovine serum albumin · CB: carbonate-bicarbonate buffer · EDA: *N*-[3-(trimethoxysilyl) propyl]ethylenediamine · NHS: *N*-hydroxysuccinimidyl · PBS: phosphate buffered saline · PDMS: poly (dimethylsiloxane) · PEG: poly (ethylene glycol) · RICM: reflection interference contrast microscopy

P. Nassoy (✉)
Laboratoire PCC, Unité Mixte de Recherches 168,
Institut Curie, 11 rue P. et M. Curie,
75005 Paris, France
E-mail: pierre.nassoy@curie.fr
Fax: +33-1-40510636

D. Cuvelier · O. Rossier · P. Bassereau · P. Nassoy
Unité Mixte de Recherches 168,
Institut Curie, 26 rue d'Ulm,
75248 Cedex 05 Paris, France

Introduction

The capability to finely control the placement and adhesion of cells on micropatterned substrates is fundamental for the development of cellular biosensors and diagnostic high-throughput assays (Mrksich and Whitesides 1995; Kane et al. 1999; Morhard et al. 2000). Attempts to design biomimetic substrates for spatially directing cellular interactions usually face two major problems: (1) the difficulty to eliminate all non-specific attractions which lead only to partial specific recognition; (2) the undesired adsorption of proteins from the culture media, which can blur the cell adhesion signals from patterned regions. Spatially localized attachment of cells therefore requires: (1) to perform a micrometer-scale patterning of the proteins of interest, (2) to properly passivate the rest of the surface against non-specific cell adhesion, (3) to ensure that adhesion of cells to functionalized patterned areas is neither enhanced by long-range generic attraction nor made ineffective by non-specific adsorption of other proteins.

Microcontact printing (μCP) represents a compelling approach to fulfilling the above-mentioned requirements. This technique has been shown to be very convenient and effective to pattern proteins by either adsorption or covalent grafting on self-assembled monolayers of alkanethiols deposited onto gold substrates (Xia and Whitesides 1998; Lahiri et al. 1999; Yan et al. 1999). Whitesides and Mrksich have also extensively studied the possibilities of guiding in situ cultured cells along defined patterns (Mrksich et al. 1996, 1997; Chen et al. 1997; Mrksich 1998). However, direct application of μCP to glass (or silica) substrates is more delicate to implement and usually leads to lower spatial resolution (Xia et al. 1995; Wang et al. 1997). A related method, namely microfluidic networks (μFN), offers an alternative

approach, which has for example found applications in the fabrication of high-resolution mosaic immunoassays on glass surfaces (Bernard et al. 2001a).

Here, we present two strategies based on μFN or the simultaneous combination of μCP and μFN to pattern "cell attractant/repellent" glass substrates. In this paper, we focus on the interaction of biotinylated red blood cells with streptavidin-patterned substrates, as a model system for cells interacting with a substrate via receptor–ligand interactions. The choice of the streptavidin–biotin complex as a receptor–ligand pair was guided by the fact that streptavidin patterned surfaces can serve as "universal" templates for further immobilization of biotinylated proteins (Wilchek and Bayer 1988). We selected red blood cells for the sake of convenience: human red blood cells are devoid of a nucleus and their composition in lipids and proteins is well known. Also, they are not motile cells [i.e. they are not actively responsive to (bio)chemical modifications of the surface]. The two methods will be first described in detail and protein patterned surfaces will be characterized. In particular, we will discuss key issues that must be addressed for achieving a proper surface passivation around bioactive patterns and inhibiting any attraction between cell and substrate other than specific ligand–receptor recognition. Finally, we will show how these biomimetic heterogeneous templates have been used to investigate the kinetics of specific attachment and spreading of individual red blood cells mediated by receptor–ligand interactions.

Materials and methods

Chemicals, proteins and cells

All buffers (phosphate buffered saline solution, PBS; carbonate-bicarbonate buffer, CB) were made up with deionized water (Millipore, 18 MΩ cm). All solvents (methanol and acetic acid) were high-performance liquid chromatography (HPLC) grade and purchased from SDS. All reagents were obtained commercially and used without further purification. We selected a silane molecule, namely *N*-[3-(trimethoxysilyl)propyl]ethylenediamine (EDA, from Sigma-Aldrich) to activate glass cover slides.

As a model receptor–ligand pair, we chose the biotin–streptavidin complex, which is known to be highly stable, easy to handle and can serve to produce universal templates for further immobilization of any kind of biotinylated adhesion molecule. Two biotinylated crosslinkers were used. In both cases, the reactive group is a *N*-hydroxysuccinimidyl (NHS) group, but the nature and length of the spacer arm are different. EZ-link-LC-LC-biotin (Pierce) is made of an 11-carbon alkyl chain, while NHS-PEG^{3400}-biotin (Shearwater Polymers) has a spacer length of about 78 poly(ethylene glycol) monomers (polydispersity index 1.02). Streptavidin was obtained from Jackson ImmunoResearch Laboratories. Passivation of non-biotinylated areas against non-specific interaction was achieved by using two blocking agents: methoxy-PEG^{5000}-NHS (kindly provided by Europa Bioproducts, UK) or bovine serum albumin (BSA, from Sigma-Aldrich). Fluorescent analogues of streptavidin and BSA, namely Cy3-Extravidin and fluorescein-BSA (Sigma-Aldrich), were used to visualize the patterned surfaces by fluorescence microscopy. Figure 1 depicts the different chemical reagents.

Fresh red blood cells were obtained from donors, washed once with PBS 290 mosmol, and three times with 0.1 M CB buffer (pH 8.5). Then, the cells were biotinylated by incubation in a 0.5 mM NHS-PEG^{3400}-biotin solution made from CB buffer for 30 min. After three washes with PBS 290 mosmol, the biotinylated cells were osmotically swollen in PBS 140 mosmol.

Fabrication of elastomeric moulds

Our strategy to design patterned surfaces was inspired from the soft lithography technique developed by Whitesides (Xia and Whitesides 1998). The first step was to fabricate soft moulds with the desired micrometer-size relief features. They were made from curing poly(dimethylsiloxane) (PDMS) (Sylgard 184, Dow Corning) at 60 °C for 4 h against photoresist masters that had the negative relief structure. Masters were prepared photolithographically by exposing and developing a photoresist pattern on customized soda-lime masks (Compugraphics, UK). The elastomeric moulds were cut from the replica, peeled off and rinsed repeatedly with ethanol and deionized water in order to wash off free polymer chains.

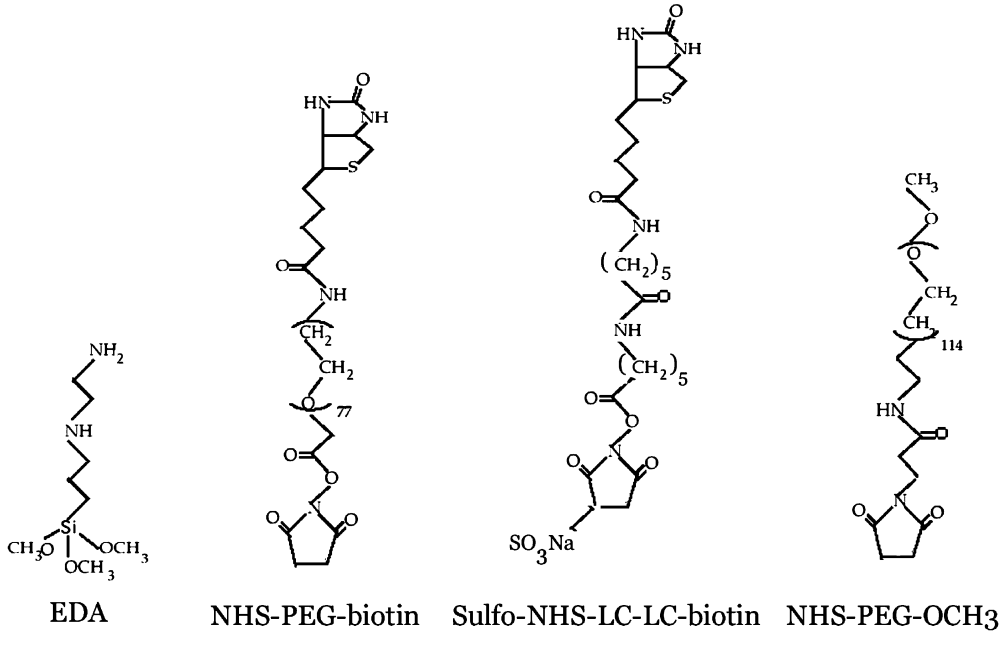

Fig. 1 Molecular structures of the amino-silane (EDA) and the three crosslinkers: NHS-PEG^{3400}-biotin, EZ-link-LC-LC-biotin, and NHS-PEG^{5000}-methoxy

Following drying under argon, the moulds were placed onto a clean glass. The channels were transversally cut at both ends to open a path for incoming liquids. Typical patterns used in this study were straight or curved lines. The dimensions were as follows: width 0.5–8 μm, depth 0.5–2 μm, and length 5–10 mm. They can be re-used up to five times after plasma treatment and extensive rinsing with ethanol.

Preparation of micropatterned surfaces

We developed two different procedures to produce glass surfaces with alternatively streptavidin-coated (i.e. attractive towards biotin) areas and inert areas (against protein adsorption and cell attachment). The first one (method 1) consists of a simultaneous dual patterning which combines the microcontact printing (μCP) and microfluidic networks (μFN) technologies: while the biotinylated crosslinker was injected into the microchannels by capillarity and was allowed to covalently bind to the pre-silanized glass slide, a blocking agent such as BSA was physisorbed on the areas in contact with a PDMS stamp previously inked with BSA. The second approach (method 2) is a two-step procedure: after initial grafting of biotin in the channels of the moulds, the rest of the surface was passivated by covalently grafting PEG.

Activation of glass surfaces with a functional silanizing agent was a preliminary requirement to implement these methods. Our silanization protocol has been described and characterized elsewhere (Merkel et al. 1999). Briefly, coverslips were first washed in a piranha solution (H_2O2/H_2SO4, 30/70), rinsed extensively with ultra-pure water, and finally with methanol. Then, silanization occurred by incubation of the glass slides in 94% acidic methanol (0.15 M acetic acid) + 4% water + 2% EDA silane. After washing with methanol and curing at 100 °C for 20 min, the resulting amino-functionalized slides were ready to use or could be stored in a desiccator for several months.

In method 1, a drop of BSA (or fluorescein-BSA) solution was applied on top of the PDMS pad for 1 h at room temperature in order to allow capture of BSA by the PDMS surface. After rinsing with water and blow-drying under argon, the pad was placed in conformal contact with a silanized coverslip. In method 2, the ''naked'' PDMS pad was directly put in contact with the amino-silanized slide. For both methods, the arrays of channels were backfilled by capillarity with a drop of solution of the biotinylated crosslinker (2 mg/mL in CB). Reaction of the NHS-terminated biotin crosslinker with the amino surface proceeded in the microchannel for 1 h. After removing quickly the PDMS pad from the surface and rinsing with ultra-pure water, the substrates were dried under a stream of argon. At this stage, substrates that were prepared following method 1 were ready to use for optical characterization and adhesion assays. In contrast, the substrates prepared following method 2 needed subsequent passivation. To do so, partially biotinylated slides were incubated in a solution of methoxy-PEG-NHS (2 mg/L in CB) for 2 h. Finally, all slides were incubated in a streptavidin solution (1 mg/mL in PBS) for 30 min by sandwiching a 200 μL drop of solution between the derivatized coverslips and soft plastic slides (Parafilm). Both routes are schematically depicted in Fig. 2.

Characterization by fluorescence microscopy

Optical characterization of the samples was carried out with an inverted microscope (Zeiss, Axiovert 200) equipped with a 100 W mercury lamp, optical filters, a 100× Plan-Achromat immersion oil objective (numerical aperture NA 1.4) and a digital monochrome camera cooled to 30 °C (Coolsnap HQ, Roper Scientific). Fluorescence images (1392×1040 pixels) were captured and analyzed with commercial software provided with the camera (MetaVue, Universal Imaging).

Adhesion assay for biotinylated red blood cells

Optical inspection of red blood cells coming in contact with the substrate was performed by reflection interference contrast microscopy (RICM) using the second camera output (1/3× CCD,

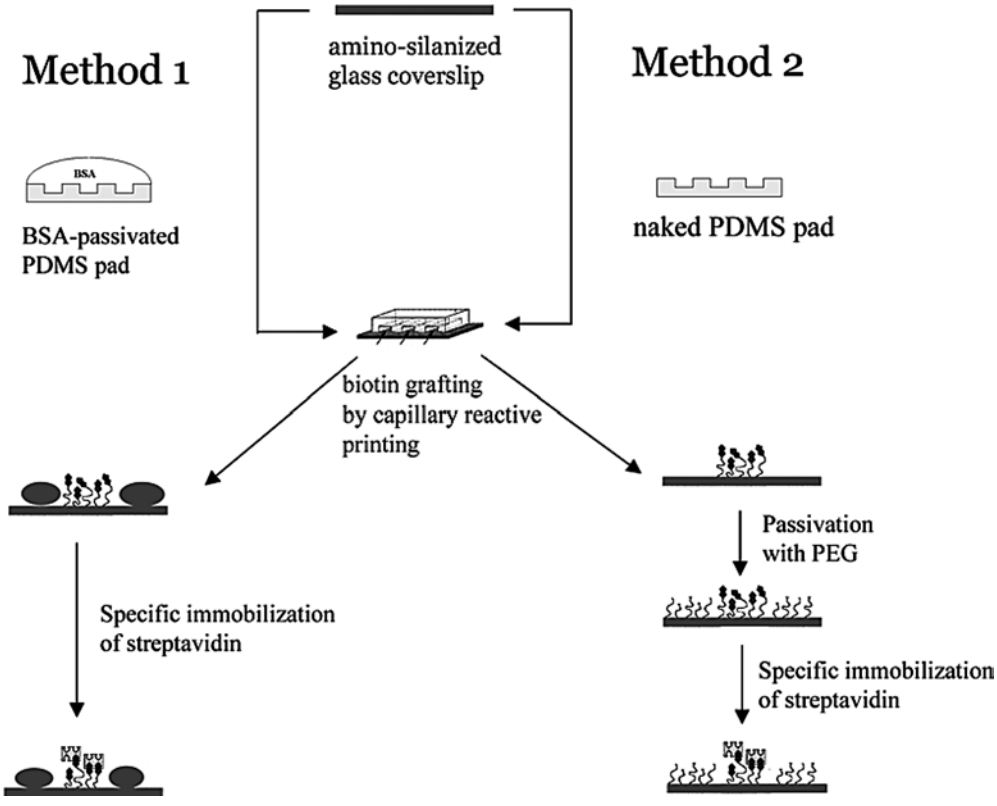

Fig. 2 Schematic representation of the two streptavidin patterning routes. Both methods use amino-silanized slides as templates and a structured PDMS pad for micropatterning. The biotinylated cross linkers are grafted to the surface by capillary reactive printing inside the microchannels moulded in the PDMS pad. In method 1, passivation of the surface is performed by simultaneous microcontact printing with the PDMS stamp inked with BSA. In method 2, the surfaces are passivated afterwards by methoxy-PEG grafting. Streptavidin is finally spatially immobilized on the biotin-derivatized lines

Pulnix PE2013) of the same microscope equipped with a narrow interferential filter ($\lambda = 546 \pm 5$ nm) and an image processor (Argus-20, Hamamatsu). Images were recorded in real time with a S-VHS tape recorder (SV0-9500MDP, Sony). After capturing the sequences of interest (Matrox Meteor-II/digital frame grabber), the stacks of images were analyzed with home-made software (kindly provided by J. Pécréaux). The contact area and profile of cells in the vicinity of the surface were derived from the interference pattern ("Newton rings") according to the image analysis described by others (Rädler and Sackmann 1993) (Fig. 3).

Results and discussion

The specificity of cell–cell or cell–matrix recognition, compared with traditional adhesive materials, lies in the interplay between electrostatic plus undulation repulsions and receptor–ligand attractions (Bruinsma et al. 1999; Weickl et al. 2002). One of the key issues in the design of biomimetic systems consists of inhibiting all kinds of generic long-range attractions (van der Waals, electrostatic, etc.). Here, we have fabricated heterogeneous surfaces that offer the following features: cell-repellent areas alternate with micrometer-scale cell-adherent areas for which attachment of cells is solely mediated by specific receptor–ligand interactions. Although many procedures are available to print ligands on solid surfaces, it is often not clear whether cell attachment is primarily mediated by long-range non-specific attractions or only by short-range specific key–lock interactions. The aim of the present work was to design biomimetic substrates for specific cell adhesion while ensuring that no long-range attraction force could interfere with the biologically relevant key–lock attraction. Careful description and characterization of the derivatized templates are presented below. Validation of our approaches was gained by using these templates to study the spreading kinetics of individual biotinylated red blood cells onto streptavidin micropatterned slides.

Non-specific adhesion of red blood cells onto unpassivated substrates may be fast and strong

Figure 4 shows RICM snapshots of an osmotically swollen erythrocyte coming in contact with an amino-silanized coverslip. In Fig. 4a, the cell was at an elevation relative to the surface higher than 200 nm. Within two video frames (80 ms), the red blood cell appeared as a large black spot, meaning that it was fully spread and in tight contact with the surface (Fig. 4b). Then, upon tension induced by adhesion, the erythrocyte burst (Fig. 4c) and was deflating, as revealed by the interference pattern corresponding to the top membrane collapsing (Fig. 4d). We observed similar ultra-fast sprea-ding of washed red blood cells when the amino-silanized slide was replaced by mercapto-, quaternary ammonium-, methyl-functionnalized slides or by naked glass. Two obvious questions then arose. (1) How may non-specific adhesion of red blood cells be inhibited? (2) Is grafting of ligands to glass enough to ensure that specific interactions become dominant over generic adhesion?

BSA or PEG coating of glass effectively prevents non-specific adhesion of red blood cells

Figure 5 displays RICM micrographs of swollen red blood cells lying on a PEG-coated surface (Fig. 5a) (obtained by covalently linking methoxy-PEG-NHS to

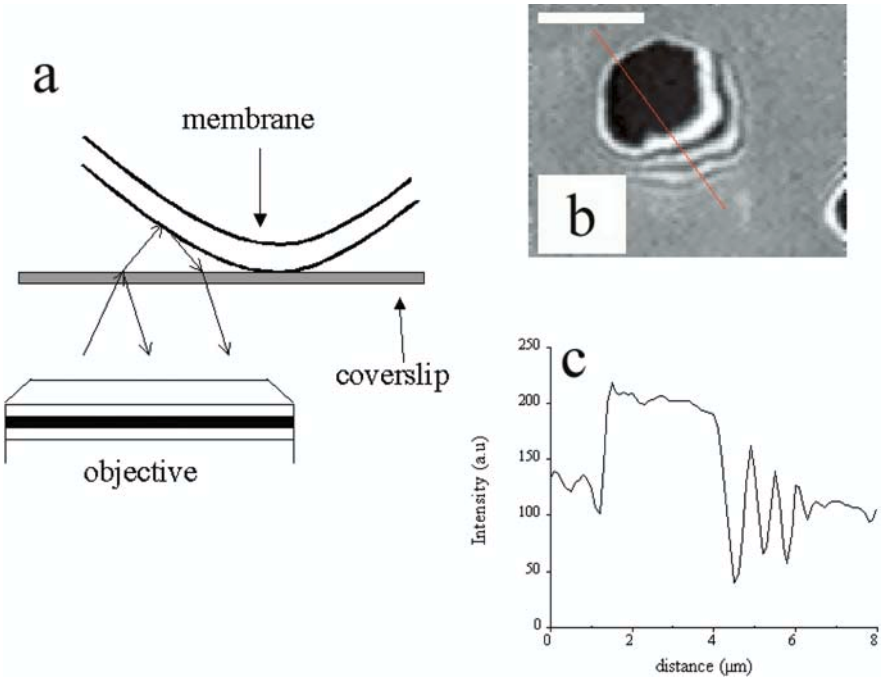

Fig. 3a–c Cell adhesion and the RICM method. (**a**) Schematic view of RICM image formation by interference of light reflected from the cell and substrate surface, respectively. (**b**) Interferogram of a red blood cell adhering to a solid substrate. The tight adhesion zone is defined by the *dark spot*. The *bar length* is 5 μm. (**c**) Intensity distribution along a radial section marked by the *red bar* in (**b**)

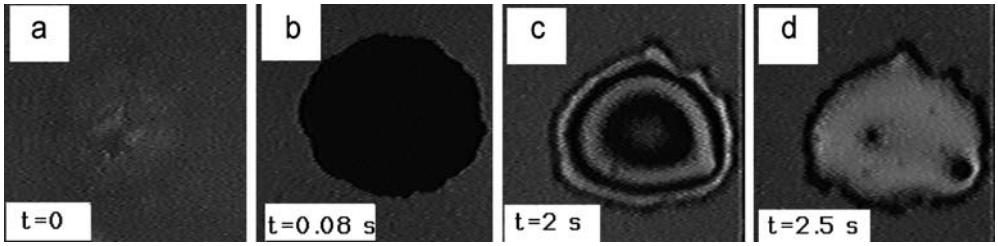

Fig. 4a–d RICM snapshots of a red blood cell on an amino-silanized coverslip. (**a**) The cell is approaching the surface. (**b**) Within two video frames, the cell is completely spread on the surface, as revealed by the *large dark disc*. (**c**) White and black interference rings correspond to the top membrane falling down after bursting of the red blood cell. (**d**) Final stage of the deflated red blood cell. The *bar length* is 5 μm

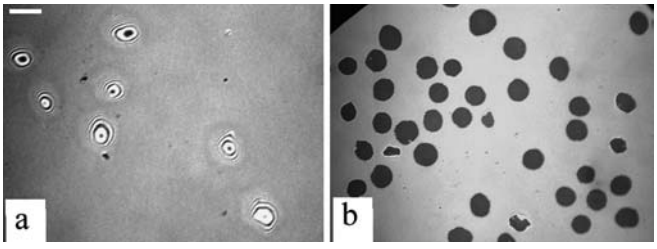

Fig. 5 RICM video micrographs of red blood cells on (**a**) PEG-passivated coverslips and (**b**) on amino-silanized coverslips. The *bar length* is 10 μm

an amino slide) and on an amino-silanized surface (Fig. 5b). On the unpassivated silanized slide, all red blood cells were fully spread, as revealed by contact area diameters of the order of the erythrocyte size (~8 μm). By contrast, areas of tight contact between cells and PEG-ylated substrates were much smaller than the projected area of the cell, typically limited to a fraction of a μm^2 up to few μm^2. These observations are consistent with many other reports which describe PEG as an effective agent against cell spreading (Lahiri et al. 1999; Papra et al. 2001; Ryan et al. 2001). Similarly, red blood cell adhesion was also very limited when the amino-functionalized substrate was first incubated in BSA solution or if BSA was added to the cell suspension. BSA is indeed known to be able to inhibit non-specific cell adhesion (Nishizawa et al. 2002). Both BSA and PEG were utilized to produce the passive areas of the micropatterned surfaces used in this work.

Immobilization of streptavidin on surfaces does not ensure specific adhesion of biotin-derivatized cells

Many chemical methods are available to print biotin on a glass surface (Hermanson et al. 1992) and the most common way to characterize the efficiency of immobilization is to test the capability of the substrate to capture streptavidin (e.g. by fluorescence microscopy or AFM) (Patel et al. 1999). Successful immobilization of streptavidin on a biotinylated surface means that specific recognition has been achieved at the molecular scale. The first difficulty that we encountered at the outset of this work was that *molecular* specific recognition might not be a sufficient condition for *cellular* specific recognition. We therefore performed adhesion assays of biotinylated red blood cells onto streptavidin-coated substrates. Different parameters were varied: (1) the nature of the biotinylated crosslinker; we either used EZ-link-LC-LC-biotin (composed of an 11-carbon alkyl spacer), or NHS-PEG^{3400}-biotin (containing a 78 ethylene glycol spacer); (2) the presence or absence of BSA in the red blood cells suspension. Native (i.e. non-biotinylated erythrocytes) were taken as a control. Adhesion tests were carried out on 300–500 red blood cells for each condition. As a clear-cut criterion for adhesion, we decided that adhesion occurred when the contact area (i.e. size of the black spot visualized by RICM) was larger than $0.5\times(\pi R_{rbc}^2) = 25\ \mu m^2$. Table 1 summarizes the main outcomes. Significant differences were noticed between the two biotinylated crosslinkers. Adhesion of red blood cells on EZ-link-LC-LC-biotin slides was not specific since native and biotinylated cells almost equally adhered. Besides, when BSA was added, adhesion was almost completely inhibited for the biotinylated or the non-biotinylated erythrocyte, indicating that this biochemical treatment of the glass surface did not prevent non-specific adsorption of BSA on top of the streptavidin layer. In contrast, when NHS-PEG-biotin was used, streptavidin-grafted slides were only an "attractant" to biotinylated cells, and the presence of BSA in solution did not alter adhesion. The presence of a PEG spacer terminated by a biotin group is clearly crucial for obtaining specific adhesion while avoiding physisorption of other proteins by screening hydrophobic or van der Waals interactions due to the silanization treatment. In the rest of this study, all cell "attractant" patterns will be obtained using NHS-PEG-biotin as a crosslinker.

Dual patterning method

We have implemented two strategies to prepare patterned substrates made of micron-size lines which are bioactive towards biotinylated red blood cells and surrounded by areas which are inert towards cell attachment and protein adsorption. Both methods have been described in the Materials and methods section and schematized in Fig. 2.

Table 1 Influence of the nature of the biotinylated crosslinker and of the presence of BSA on the specificity of red blood cell adhesion. The percentage of adhesion represents the number of red blood cells which are in close contact with the surface over more than 25 μm^2

Chemical treatment of the glasscover slide	Percentage of adhesion of biotinylated red blood cells	Percentage of adhesion of non-biotinylated red blood cells
EZ-link-LC-LC-biotin + streptavidin	98%	88%
NHS-PEG-biotin + streptavidin	97%	11%
EZ-link-LC-LC-biotin + streptavidin + BSA in solution	15%	9%
NHS-PEG-biotin + streptavidin + BSA in solution	94%	7%

Briefly, method 1 combines in one step the basics of two existing techniques, namely μCP and μFN. On the one hand, the ligand of interest (here, biotin) was printed onto glass by performing a microreaction inside the channels (molded by soft lithography) of an amino-reactive PEG-biotin to the amino-silanized surface. This approach is very similar to the μFN technique, which has been widely exploited by the group in Zürich (Delamarche et al. 1997; Bernard et al. 2001a). On the other hand, areas which were in contact with the PDMS pad could be passivated by transfer of BSA from the stamp to the slide by the usual μCP technique, which was developed by Whitesides' group (Mrksich and Whitesides 1995; Xia and Whitesides 1998). Figure 6a shows a two-color fluorescence video-micrograph of a patterned glass slide with lines of "red" (Cy3-labeled) streptavidin surrounded by "green" (fluorescein-labeled) BSA. This photograph qualitatively indicates that BSA and streptavidin were mainly detected at the desired location with a good spatial definition. Sometimes, possible defects were revealed. They were due to bad alignment of the mask during the lithographic fabrication of the photoresist master or to the presence of dust on the surface of the PDMS pad.

Method 2 consists of first performing capillary reactive printing of PEG-biotin using the μFN technique. In a second step, prior to streptavidin coating, the rest of the surface was passivated by grafting methoxy-PEG-NHS. Figure 6b displays a fluorescence video-micrograph of "red" streptavidin patterned slides when methoxy-PEG was used for passivation. For comparison, Fig. 6c shows a fluorescence micrograph of streptavidin patterned slides when the amino slide was not passivated. In both cases, biotin-modified lines were clearly detected. However, the difference in signal/noise ratios was significant. When the passivation step using PEG was included in the protocol, we found that the S/N ratio increased from 2.5 ± 1 to around 8 ± 1. A similar quantitative analysis of the contrast level for slides prepared following method 1 yielded $S/N = 7 \pm 1$. Also interesting, we note that the fluorescence intensity was very homogeneous along one line and between different lines, as long as the width of the lines was larger than 2 μm. Figure 6d shows "red" strepatvidin patterns made of straight lines of 500 nm in width and prepared according to method 2. In this case, significant variations of the fluorescent intensity across the surface and reduced S/N ratios were observed. An increase of the PEG-biotin concentration (up to 10 mg/mL) did not lead to any marked improvement. We suggest that the enhanced heterogeneity in streptavidin density might result from decreased reactivity of the biotinylated crosslinker in conditions of sub-micronic confinement.

Before evaluating our "repellent/bioactive" patterned slides versus specific cell attachment, we wish to point out several important aspects about the novelty of these approaches. First, both methods were designed to be applied to glass substrates. To our knowledge, most protein patterning strategies have been successfully developed on gold or polymeric substrates (Xia and Whitesides 1998; Hyun et al. 2002; Tan et al. 2002). A few remarkable exceptions, where silicon wafers or oxidized PDMS were used as templates, come from the group in Zürich (Bernard et al. 2001b) and more recently from others (Chen et al. 2002). Yet glass is not widely utilized because of the difficulty in printing silanes by μCP with high spatial resolution (Xia et al. 1995; Wang et al. 1997). We were able to overcome this problem by activating the whole glass slide with a silanized agent *prior to* the patterning step. Here, the key point lies in the fact that contact between the PDMS stamp and the substrate did not need to be very tight, as is required for the classical μCP technique. Although hydrophobized silane-modified slides are less adhesive to PDMS than plasma-treated slides, microfluidic channels could be gently backfilled by capillarity while avoiding any leak of fluid.

Second, concerning method 2, we combined the existing μFN technology to graft biotin with the remarkable capability of PEG to inhibit protein adsorption and cell attachment. Here, the choice of the biotinylated crosslinker was crucial. As discussed previously, the use of a PEG spacer terminated with a biotin group enabled us to avoid any non-specific cell adhesion and to render the derivatized pattern solely adherent via specific receptor–ligand interaction.

Third, we believe that method 1 offers a new, simple and rapid approach to perform dual patterning of glass substrates in one step. We have shown that μCP and μFN could be advantageously used simultaneously to adsorb a protein by transfer from the PDMS stamp and to graft another protein inside the channel arrays of the PDMS mould.

From the viewpoint of hereafter-mentioned cell adhesion assays, no difference was noted between the two methods. All the results reported below were obtained using slides prepared according to both approaches.

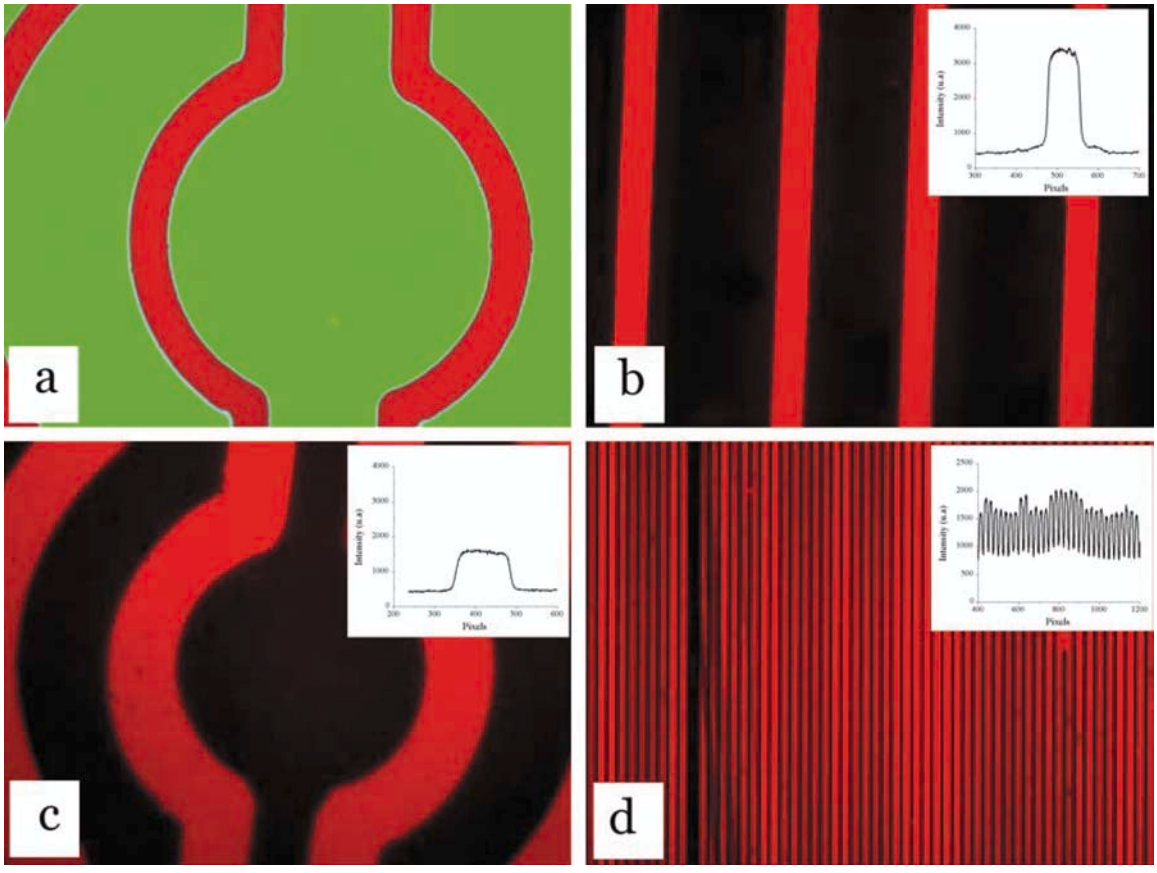

Fig. 6a–d Fluorescence micrographs of streptavidin patterned surfaces. (**a**) ''Red'' streptavidin lines (3 μm in width) surrounded by ''green'' BSA passivated areas (method 1). (**b**) ''Red'' streptavidin lines (3 μm in width) surrounded by methoxy-PEG passivated areas (method 2). (**c**) Biotin lines (6 μm in width) surrounded by amino-silanized (i.e. unpassivated) areas and detected by ''red'' streptavidin. (**d**) Sub-micronic ''red'' streptavidin lines (500 nm in width) separated by 500-nm wide PEG-ylated lines. The *insets* are linescans of the fluorescence intensity distribution

Interaction of biotinylated red blood cells with streptavidin micropatterned substrates

Adhesion tests consisted of depositing a suspension of biotinylated red blood cells onto streptavidin/BSA (or streptavidin/PEG) patterned slides modified following method 1 (or method 2). No flow is applied and the cells come in contact with the substrate due to gravity. Figure 7a shows the superposition of a fluorescence micrograph and a RICM micrograph of the same region of the patterned slide once the biotinylated red blood cells were sedimented. Here, streptavidin lines, which were detected by fluorescence using Cy3-Extravidin, were 4 μm in width, i.e. slightly smaller than the diameter of a red blood cell. RICM allowed visualization of the contact area of the erythrocytes with the coverslip. As shown in Fig. 7a, we observe that large contact areas (meaning that red blood cells are spread and strongly adhere to the substrate) are co-localized with streptavidin patterns. In contrast, blood cells were weakly adhered (if not sit only) on the passivated areas. This differential adhesion was confirmed by increasing the density of red blood cells on the surface and dipping the coverslip in fresh PBS. Figure 7b displays a RICM video-micrograph after washing. All remaining red blood cells are only found along streptavidin lines. Cellular ''wires'' are thus formed. More interesting, we also observe that red blood cells are slightly deformed, since the contact area is often found to deviate from round shape. The magnification in Fig. 7c shows biotinylated red blood cells which overlap a streptavidin line and a passivated area. Within one cell, the contact area clearly stops at the border. In a last experiment, when the width of streptavidin lines is decreased down to sub-micronic dimensions, the morphology of adhering red blood cells is strikingly different. Figure 7d shows a RICM mircograph obtained on 500-nm wide streptavidin lines separated by 500 nm PEG areas. Tight contact is observed on streptavidin lines while the cell membrane is suspended between two adhesive lines. Besides, red blood cells become deformed by a digitation process. Membrane ''fingers'' can grow along adherent lines. When all these adhesion assays are taken together, we can conclude that cell attachment is highly localized and specific.

At this stage, note that the present work is somehow different from other works which reported possible *cell guidance* along patterned surfaces (Mrksich et al. 1996, 1997; Mrksich 1998; Kane et al. 1999; Takayama et al.

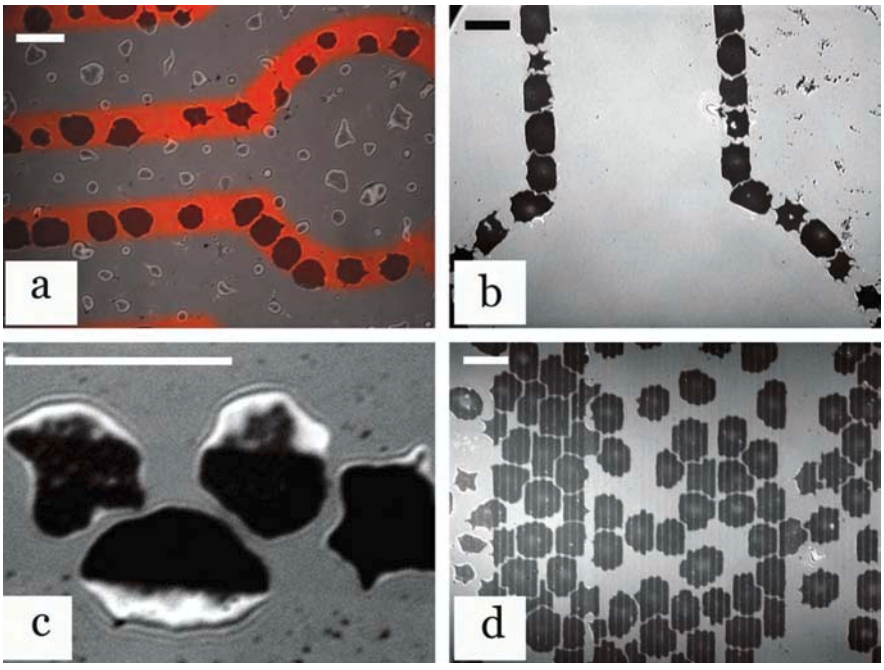

Fig. 7a–d Video micrographs of biotinylated red blood cells on streptavidin patterned surfaces. (**a**) Superposition of two images taken in the fluorescence and RICM modes. Patterned lines are 8 μm in width. (**b**) RICM image after removing all weakly adhering red blood cells by washing. Cellular "wires" are co-localized with streptavidin patterns. (**c**) Magnification of a RICM image at the border between a streptavidin line and a passivated area. Red blood cells overlap the two regions but only adhere specifically to the streptavidin-coated zone. (**d**) RICM image of red blood cells adhering onto sub-micronic patterned substrates (width 500 nm). Each *bar* is 10 μm in length

1999; Nishizawa et al. 2002). In the latter case, surfaces were designed so that a differential adhesivity was created between patterned areas. After seeding cells on one side of the surface, moving cells (like fibroblasts) grow and prefer to spread onto one type of chemically modified pattern instead of covering "unfavorable" areas. Yet, in many cases, there is no clear evidence that cells would not stick in a non-specific manner to the supposedly passivated regions. In the present study, red blood cells (which are incapable of any active movement) were "seeded" everywhere on the patterned substrate, but their attachment was found to be restricted to the desired regions.

Spreading kinetics of individual red blood cells on micropatterned substrates

In the previous section, we have given a static description of biotinylated red blood cells in contact with patterned "attractant/repellent" surfaces. However, we have also examined the spreading kinetics of individual red blood cells on the same surfaces in order to obtain additional hints about the nature of cell–substrate interactions. Our results on red blood cells have eventually been compared to the theoretical model proposed by Boulbitch and co-workers for modeling the specific adhesion of decorated vesicles (Boulbitch et al. 2001).

Figure 8 shows snapshots of the spreading process of a biotinylated red blood cell on a strepatvidin line that is wider than R_{rbc}. Initially, the red blood cell was not in contact with the substrate (Fig. 8a). In Fig. 8b, the nucleation of a small domain of tight adhesion occurs. Then, the contact area increases gradually (Fig. 8c), expanding until the whole contact zone is tightly adhered

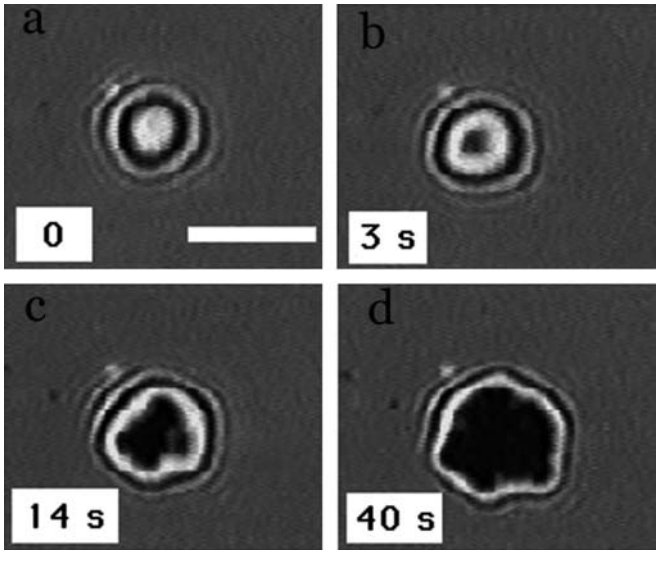

Fig. 8a–d Time sequence of the spreading of a biotinylated red blood cell on a streptavidin-coated surface as seen by RICM. The bar represents 5 μm. (**a**) The red blood cell is not in contact with the surface. (**b**) Nucleation of the state of the tight adhesion. (**c**, **d**) Different stages of the expansion of the tight adhesion state

(Fig. 8d). This process is therefore strongly reminiscent of a first-order transition as observed in wetting phenomena (Bruinsma and Sackmann 2001) or phase separation (Komura and Andelman 2000). The time from contact initiation until complete spreading depends upon the surface density of biotin groups on the red blood cells and varies from ~10 s to 1 min. The growth process of the area of adhesion has been monitored by image processing. In the time sequence shown in Fig. 8, the zone of tight adhesion has approximately a circular shape, although not perfectly regular. Yet, many other scenarios

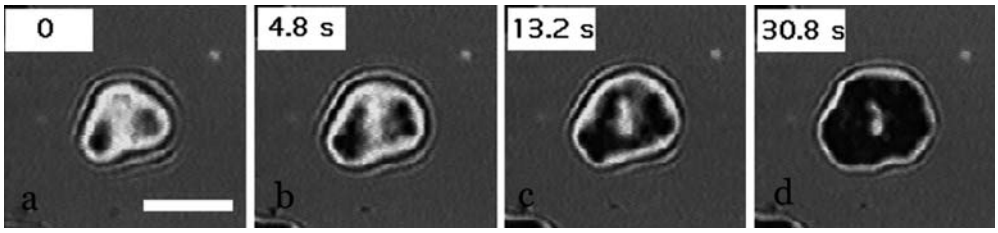

Fig. 9a–d Time sequence of the spreading of a biotinylated red blood cell on a streptavidin-coated surface as seen by RICM. The bar represents 5 μm. (**a**) Two nucleation centers are formed. (**b**, **c**, **d**) Different stages of the expansion of the tight adhesion zones. A blister of non-adhering membrane is trapped close to the center of the cell (**d**)

were also observed. As shown in Fig. 9a–d, two or more adhesion patches can be formed and grow simultaneously until they merge while leaving some trapped blisters (white spots) of unadhered membranes. This kind of growth process was discarded from our analyses. More subtle, if a single adhesion nucleus was created close to the centre of the cell, it was found to grow most often isotropically (Fig. 8a–d), while if the nucleus was created close to the edge of the cell or at a border between a streptavidin line and a passive area, the adhesion patch was pinched on one side and could only propagate in the opposite direction. Finally, we also observed hybrid processes for which the adhesion nucleus started to grow in an isotropic way before being directed. Consequently, derivation of the time evolution of the adhesion front from the measure of the contact area following $\xi(t)=[A(t)/\pi]^{1/2}$ was likely to induce some bias in the estimate of the propagation velocity of the front. For comparison of our experimental results with the one-dimensional model developed by Boulbitch et al. (2001), we had to check the influence of these different modes of propagation of the adhesion front. To do so, in one series of experiments we performed systematic monitoring of the displacement of the adhesion patch centre. Figure 10 displays two different scenarios. In Fig. 10a, growth is almost isotropic with no overall significant displacement of the centre of the adhesion zone. In this case, the propagation front was indeed obtained from the relation $\xi(t)=[A(t)/\pi]^{1/2}$. In contrast, Fig. 10b is an example where the very beginning of the growth is roughly isotropic until about 5 s. Afterwards, propagation was basically unidirectional. Front propagation could then be either derived from the position of the adhesion patch centre or from $\xi(t)=A(t)/w$, where w is the constant width of the growing adhesion patch. This approach allowed us to eliminate all artefacts that would be resulting of a global ''blind'' image analysis. However, in order to gain sufficient statistics for the spreading kinetics of red blood cells, in a second series of experiments we finally bypassed this tedious manual analysis by taking benefit of the preparation of sub-micronic patterns described above. Figure 11 shows a typical scenario of biotinylated red blood cell adhesion on 500-nm wide streptavidin lines separated by 500 nm PEG areas. The pattern width being

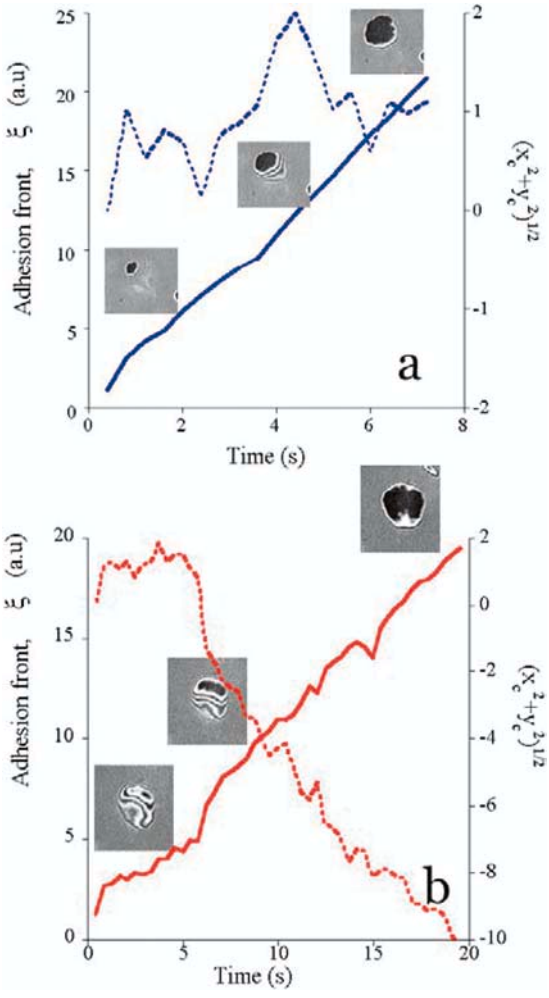

Fig. 10a, b Displacement of the adhesion front, ξ (*solid lines*), and of the center of the adhesion zone, $(x_c^2+y_c^2)^{1/2}$ (*dashed lines*), versus time for two different scenarios. (**a**) Isotropic growth of the adhesion nucleus. The centre of the adhesion zone is not moving. (**b**) Directional growth of the adhesion nucleus. This is revealed by the overall displacement of the center of the adhesion zone. Spatial units are in pixels. Photographs which are displayed in inset show the state of the adhering red blood cells

far below the size of a red blood cell, adhesion front propagation occurred almost ideally along one direction. The snapshots were taken when one adhesion ''stripe'' was already formed. The initial time was chosen when the adhesion zone jumped to the closest line and started to propagate. Direct measure of the adhesion zone length with time gives $\xi(t)$.

With all experiments on both wide and narrow lines are taken together, the kinetics of red blood cells adhe-

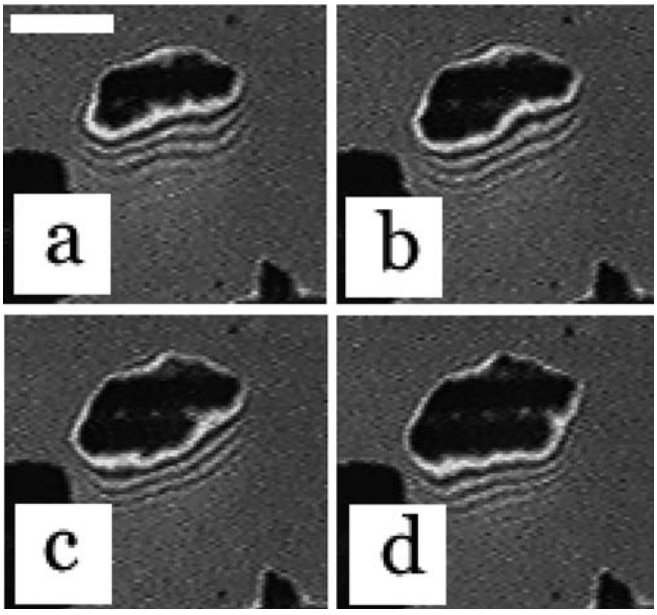

Fig. 11a–d RICM snapshots of a biotinylated red blood cell in contact with a streptavidin patterned surface. Patterns are 500 nm wide lines. At time $t = 0$, the red blood cell has already adhered to one streptavidin-decorated stripe. Photographs **a**–**d** show the propagation of the front along the second adhesive stripe. Two successive images are separated by one second. The *scale bar* represents 5 μm

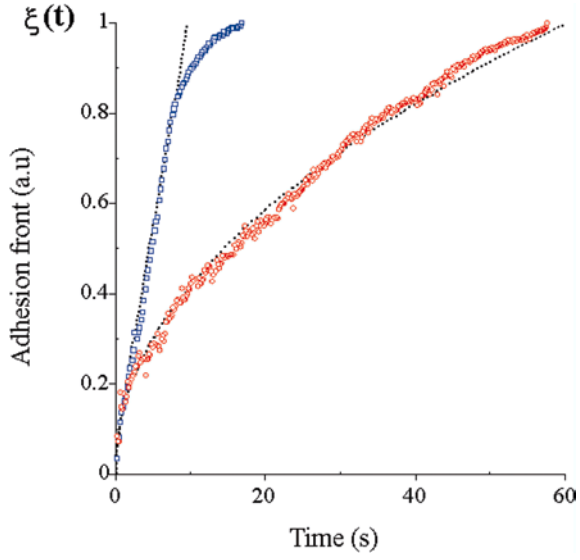

Fig. 12 Typical displacement curve of the front of adhesion versus time for low (*red circles*) and high (*blue squares*) level of biotinylation of the red blood cells. The motion of the front was determined by measuring the length of adhesion stripes by the image processing. For high biotin concentration the displacement increases linearly with t almost up to the end of the adhesion zone. For the lower biotin concentration the front displacement exhibits a square-root regime ($\xi \propto t^{1/2}$). The *dashed lines* show the corresponding fits

sion mediated by biotin–streptavidin interaction was investigated on 50–70 cells for two conditions of biotin density on the erythrocytes: low biotinylation level (corresponding to a 2 min incubation of the cell suspension in NHS-PEG-biotin) and high biotinylation level (corresponding to a 20 min incubation of the cell suspension in NHS-PEG-biotin). The time evolution of the adhesion front position (normalized by the maximal adhesion length) for low and high biotinylation levels is displayed in Fig. 12. Complete spreading of red blood cells was faster at high biotin concentrations. More importantly, two regimes corresponding to the two concentrations in biotin could be distinguished. At low biotin concentration, the front motion is found to vary as $t^{1/2}$. In the regime of high biotin concentration, the front initially moves at constant velocity ($\xi \propto t$). At longer times, when ξ approaches $2 \times R_{\mathrm{rbc}}$, its motion is slowed down and stops within about 10 s.

Quantitative and detailed description of the curves in Fig. 12 can be achieved by analyzing our experiments in the framework of Boulbitch's theory (Boulbitch et al. 2001). We begin by briefly reviewing the pertinent features of the theoretical models.

1. At a low concentration of ligands (i.e. biotin groups on the red blood cells), the front motion is dominated by diffusion. Propagation of the adhesion zone results from the diffusion of the biotinylated proteins from the free membrane to the front and from the binding-unbinding reaction between mobile biotinylated proteins (L) and immobilized streptavidin (R). This gives:

$$\xi = \alpha\sqrt{t} \tag{1}$$

and the prefactor α is defined by:

$$\alpha \approx k_{+}^{2\mathrm{D}} b^2 \frac{(c_{\mathrm{bio}} - K_{\mathrm{d}})}{\sqrt{\pi D}} \tag{2}$$

where $k_{+}^{2\mathrm{D}}$ (expressed in $\mathrm{m^2\ s^{-1}}$) is the forward reaction rate for $\mathrm{L + R \rightarrow LR}$, b is the width of the reaction zone, c_{bio} (expressed in $\mathrm{m^{-2}}$) is the surface number density of mobile biotin groups at the surface of the red blood cells, K_{d} (in $\mathrm{m^{-2}}$) is the dissociation constant of the reaction $\mathrm{L + R \rightarrow LR}$, and D is the coefficient diffusion of the biotinylated proteins.

2. At a high concentration of ligands (i.e. biotin groups on the red blood cells), the front motion is dominated by reaction between ligands and receptors. Diffusion is negligible. Yet the association rate of the reaction is limited by the expulsion of lipopolymers (glycocalix) out of the adhesion zone. $k_{+}^{2\mathrm{D}}$ is therefore weighted by a Boltzmann factor, $\exp(-\Pi A_{\mathrm{strep}}/\mathrm{k_B T})$, where Π is the lateral osmotic pressure difference of the lipopolymers and $1/A_{\mathrm{strep}}$ is the surface density of streptavidin molecules on the substrate. In the perfect gas approximation, $\Pi = \mathrm{c_{glycocalix} kBT}$. The velocity of the adhesion front then becomes:

$$\frac{\mathrm{d}\xi}{\mathrm{d}t} = b c_{\mathrm{strep}} k_{+}^{2\mathrm{D}} \exp\left(-c_{\mathrm{glycocalix}} A_{\mathrm{strep}}\right) \tag{3}$$

and is found to be independent of the concentration of biotinylated proteins.

We have already noticed that our experimental data are in good qualitative agreement with the theoretical models. This tends to indicate that attachment and spreading of biotinylated erythrocytes is indeed solely due to specific biotin–streptavidin interactions. In order to push the analysis further, and to determine whether the spectrin network underlying the red blood cell membrane has an influence on the spreading kinetics, we need to give estimates of the different relevant parameters.

The 2D association constant of the streptavidin–biotin complex can be derived from the knowledge of $K_d^{3D} = 10^{-15}$ M/L $= 10^{-12}$ M/m^3 $= 6\times10^{11}$ molecules/m^3 (Green 1975) and from the 2D dissociation rate, $k_-^{2D} = 1/44h = 6\times10^{-6}$ s^{-1}, which has been measured previously (Merkel et al. 1999). By expressing $K_d^{2D} = k_-^{2D}/k_+^{2D} \approx K_d^{3D} d_r$ (with d_r being the characteristic thickness in which the reaction takes place; $d_r \approx 10$ nm), we obtain: $k_+^{2D} = 10^9$ m^2 s^{-1}. The density of biotin-labeled proteins at the surface of red blood cells, c_{bio}, can be easily estimated since most abundant membrane proteins which are likely to be biotinylated are band 3 proteins. Biochemical studies have shown that each red blood cell has about 10^6 copies (Mohandas and Evans 1994), meaning that the surface number density is 5×10^{15} m^{-2}. If one assumes that labeling efficiency is directly proportional to the incubation time of red blood cells in the solution of biotinylated crosslinker, and that saturation is obtained for 20 min incubation time, one may take $c_{bio} = 5\times10^{15}$ m^{-2} at high biotinylation levels, and $c_{bio} = 5\times10^{14}$ m^{-2} at low biotinylation levels. As a consequence, for both regimes, $c_{bio} >> K_d^{2D} = 6\times10^2$ m^{-2}. Equation (1) is then reduced to:

$$\alpha \approx k_+^{2D} b^2 \frac{c_{bio}}{\sqrt{\pi D}} \tag{4}$$

Also, the coefficient diffusion of band 3 proteins has been measured by single-particle tracking and fluorescence recovery after photobleaching and was found equal to 10^{-11} m^2 s^{-1} (Golan and Veatch 1980). The surface density of streptavidin molecules on glass surfaces was kept constant and was measured by fluorescence-assisted cell sorting (data not shown): $c_{strep} = 3\times10^{16}$ m^{-2}. The projected area of a streptavidin molecule is 25 nm^2. More difficult is the evaluation of $c_{glycocalix}$. For red blood cells, the glycocalix is mainly composed of glycolipids (about 5×10^7 per cell, i.e. 2.5×10^{17} molecules m^{-2}). The only remaining unknown parameter is b, the width of the reaction zone, which might be expected to be in the 1–10 nm range (Boulbitch et al. 2001).

Experimentally, in the diffusion-dominated regime, the coefficient α is found equal to 0.6 ± 0.2 μm s$^{-1/2}$, which fits with the theoretical value provided that we set $b = 2.5$ nm. Note that, incidentally or not, 2.5 nm is the size of one streptavidin binding pocket. In the reaction-dominated regime, the velocity of adhesion front is found to be equal to 0.55 ± 0.18 μm s^{-1}. This value is in good agreement with the theoretical prediction provided that $c_{glycocalix} = 5.6 \pm 10^{17}$ m^{-2}, while we proposed $c_{glycocalix = 2.5 \pm 10^{17}}$ m^{-2} as a coarse approximation.

More important than the absolute values of these parameters, the main outcome lies in the fact that our experimental observations with erythrocytes can be rationalized by theoretical models which describe cell spreading as only mediated by specific ligand–receptor interactions. In other words, although indirect, this is a clear piece of evidence that the biomimetic substrates prepared as described above are well passivated against generic cell adhesion. Besides, the design of nearly one-dimensional patterns (relative to the size of the erythrocytes) provides a straightforward and convenient way to monitor the attachment kinetics of cells on decorated substrates. Our approach was validated for the biotin–straptavidin complex but could be extended to many other ligand–receptor pairs by simply immobilizing biotinylated proteins on these strepatvidin-coated templates.

Furthermore, our results on red blood cells can be compared with those obtained by Boulbitch et al. (2001) for the adhesion of a model biomimetic system, namely RGD vesicles on integrin-covered substrates. Both diffusion- and reaction-dominated regimes were also observed. Values for α were found in the 0.15–0.35 μm s$^{-1/2}$ range, depending upon RGD concentration. At the first sight, we may note a good agreement in terms of order of magnitude between their values and ours. Yet, quite surprisingly, the diffusion-limited motion of the adhesion front is faster for biotinylated red blood cells on streptavidin-coated substrates. Naively, we could expect an opposite trend, since membrane proteins on red blood cells are not completely free to diffuse. Single-particle tracking experiments have shown that the lateral diffusion of band 3 proteins is restricted because of confinement in membrane skeletal "corrals" (Golan, unpublished results). However, we believe that this confinement effect is irrelevant here. Indeed, the typical size of confinement areas is on the order of 100 nm, which is much larger than the characteristic length of the zone over which the receptor–ligand reaction occurs ($b = 2.5$ nm). Close to the adhesion front, everything happens as if proteins were freely diffusing. Moreover, the biotin–streptavidin complex has the peculiarity of being very stable. This explains why we could neglect any dissociation process within the course of front propagation. In contrast, the assumption $K_d << c_{ligand}$ is not valid for the more labile RGD-integrin pair, which may account for a lower value of the α prefactor. Concerning the reaction-dominated regime, we have found a propagation velocity of the adhesion front of 0.55 μm s^{-1}, which is in the 0–3 μm s^{-1} range reported by the German group (Boulbitch et al. 2001) over a large variation of concentration in lipopolymers and ligands.

In summary, we have described two methods for creating cell "attractant/repellent" patterns on glass surfaces, from a few microns scale down to 500 nm. Our approaches involve μCP and/or μFN techniques in a relatively unusual manner and extend the patterning to

glass substrates that are widely used in biology and biophysics related fields. The ligand of interest (biotin) was grafted at controlled locations on activated glass by reaction in the channels of a structured PDMS mould placed in contact with this substrate. Passivation of the surface against cell non-specific adhesion was obtained either by μCP of BSA or by subsequent PEG grafting. We have also demonstrated that the choice of the biotinylated crosslinker is crucial for effective specific cell adhesion. We especially pointed out the need (and difficulty) to suppress any kind of long-range generic attraction forces. Our patterned substrates exhibit a high contrast for specific adhesion and non-specific adhesion is mostly inhibited. We believe that this further improvement in surface patterning using glass coverslips as substrates is very promising for biotechnological applications.

Finally, after optimization of our patterned templates, we have studied the dynamics of the adhesion and spreading of erythrocytes labeled with biotin groups on localized strepatvidin-covered regions of glass cover slides. We have shown that the growth of the adhesion zone exhibits two distinct regimes depending upon the concentration of ligands on the cell surface, in good agreement with the theoretical model of Boulbitch at al (Boulbitch et al. 2001). Our results are the first experimental confirmation using real cells and not decorated vesicles of this model. It is in fact a first step for understanding the recruitment of adhesive molecules independently of any interaction with the cellular cytoskeleton and any reorganization. For more complex cells, the role of the cytoskeleton and of the internal signaling will have to be incorporated.

Acknowledgements We thank Axel Buguin for his advice on lithography, Françoise Brochard-Wyart for stimulating discussions, and Jacques Prost for supporting our ongoing project. The work was supported by the CNRS through the ACI ''Physicochimie de la Matière Complexe 2000'' and ''Nano-Objet Individuel 2001'' programs as well as by a grant from the La Ligue Nationale contre le Cancer (N/ref. 75/01-RS/83). One of us (O.R.) thanks the ARC for the one-year fellowship (no. Ml/MLD/CM-P01/5). We also received generous help from the Institut Curie.

References

Bernard A, Michel B, Delamarche E (2001a) Micromosaic Immunoassays. Anal Chem 73:8–12

Bernard A, Fitzli D, Sonderegger P, Delamarche E, Michel B, Bosshard HR, Biebuyck H (2001b) Affinity capture of proteins from solution and their dissociation by contact printing. Nat Biotechnol 19:866–869

Boulbitch A, Guttenberg Z, Sackmann E (2001) Kinetics of membrane adhesion mediated by ligand–receptor interaction studied with a biomimetic system. Biophys J 81:2743–2751

Bruinsma R, Sackmann E (2001) Bioadhesion and the dewetting transition. CR Acad Sci Paris 2:803–815

Bruinsma R, Behrisch A, Sackmann E (1999) Adhesive switching of membranes: experiment and theory. Phys Rev E 57:2123–2128

Chen CS, Mrksich M, Huang S, Whitesides GM, Ingber DE (1997) Geometric control of cell life and death. Science 276:1425–1428

Chen JY, Klemic JF, Elimelech M (2002) Micropatterning microscopic charge heterogeneity on flat surfaces for studying the interaction between colloidal particles and heterogeneously charged surfaces. Nano Lett 2:393–396

Delamarche E, Bernard A, Schmid H, Michel B, Biebuyck H (1997) Patterned delivery of immunoglobulins to surfaces using microfluidic networks. Science 276:779–781

Golan DE, Veatch W (1980) Lateral mobility of band 3 in the human erythrocyte membrane studied by fluorescence photobleaching recovery: evidence for control by cytoskeletal interactions. Proc Natl Acad Sci USA 77:2537–2541

Green NM (1975) Avidin. Adv Protein Chem 29:85–133

Hermanson GT, Krishna Mallia A, Smith PK (1992) Immobilized affinity ligand techniques. Academic Press, New York

Hyun J, Ma H, Banerjee P, Cole J, Gonsalves K, Chilkoti A (2002) Micropatterns of a cell-adhesive peptide on an amphiphilic comb polymer film. Langmuir 18:2975–2979

Kane RS, Takayama S, Ostuni E, Ingber DE, Whitesides G (1999) Patterning proteins and cells using soft lithography. Biomaterials 20:2363–2376

Komura S, Andelman D (2000) Adhesion induced lateral phase separation in membranes. Eur Phys J E 3:259–271

Lahiri J, Ostuni E, Whitesides GM (1999) Patterning ligands on reactive SAMs by microcontact printing. Langmuir 15:2055–2060

Merkel R, Nassoy P, Leung A, Ritchie K, Evans E (1999) Energy landscapes of receptor–ligand bonds explored with dynamic force spectroscopy. Nature 397:50–53

Mohandas N, Evans EA (1994) Mechanical properties of the red cell membrane in relation to molecular structure and genetic defects. Annu Rev Biophys Biomol Struct 23:787–818

Morhard F, Pipper J, Dahint R, Grunze M (2000) Immobilization of antibodies in micropatterns for cell detection by optical diffraction. Sens Actuators B 70:232–242

Mrksich M (1998) Tailored substrates for studies of attached cell culture. Cell Mol Life Sci 54:653–662

Mrksich M, Whitesides GM (1995) Patterning self-assembled monolayers using microcontact printing: a new technology for biosensors? Trends Biotechnol 13:228–235

Mrksich M, Dike LE, Tien JY, Ingber DE, Whitesides GM (1996) Controlling cell attachment on contoured surfaces with self-assembled monolayers of alkanethiolates on gold. Proc Natl Acad Sci USA 93:10775–10778

Mrksich M, Dike LE, Tien JY, Ingber DE, Whitesides GM (1997) Using microcontact printing to pattern the attachment of mammalian cells to self-assembled monolayers of alkanethiolates on transparent films of gold and silver. Exp Cell Res 235:305–313

Nishizawa M, Takoh K, Matsue T (2002) Micropatterning of HeLa cells on glass substrates and evaluation of respiratory activity using microelectrodes. Langmuir 18:3645–3649

Papra A, Bernard A, Juncker D, Larsen NB, Michel B, Delamarche E (2001) Microfluidic networks made of poly(dimethylsiloxane), Si and Au coated with polyethylene glycol for patterning proteins onto surfaces. Langmuir 17:4090–4095

Patel N, Sanders GHW, Shakesheff KM, Cannizzaro SM, Davies MC, Langer R, Roberts CJ, Tendler SJB, Williams PW (1999) Atomic force microscopy analysis of highly defined protein patterns formed by microfluidic networks. Langmuir 15:7252–7257

Rädler J, Sackmann E (1993) Imaging optical thicknesses and separation distances of phospholipid vesicles at solid surfaces. J Phys II (France) 3:727–748

Ryan PL, Foty RA, Kohn J, Steinberg MS (2001) Tissue spreading on implantable substrates is a competitive outcome of cell–cell vs. cell–substratum adhesivity. Proc Natl Acad Sci USA 98:4323–4327

Takayama S, McDonald JC, Ostuni E, Liang MN, Kenis PJA, Ismagilov RF, Whitesides GM (1999) Patterning cells and their environments using multiple laminar fluid flows in capillary networks. Proc Natl Acad Sci USA 96:5545–5548

Tan JL, Tien J, Chen CS (2002) Microcontact printing of proteins on mixed self-assembled monolayers. Langmuir 18:519–523

Wang D, Thomas SG, Wang KL, Xia Y, Whitesides GM (1997) Using an elastomeric phase mask for sub-100 nm photolothography in the optical near-field. Appl Phys Lett 70:2658–2660

Weikl TR, Andelman D, Komura S, Lipowsky R (2002) Adhesion of membranes with competing specific and generic interactions. Eur Phys J E 8:59–66

Wilchek M, Bayer EA (1988) The avidin–biotin complex in bioanalytical applications. Anal Biochem 171:1–32

Xia Y, Whitesides GM (1998) Soft lithography. Angew Chem Int Ed 37:550–575

Xia Y, Mrksich M, Kim E, Whitesides GM (1995) Microcontact printing of octadecysiloxane on the surface of silicon dioxide and its application in microfabrication. J Am Chem Soc 117:9576–9577

Yan L, Huck WTS, Zhao X-M, Whitesides GM (1999) Patterning thin films of poly(ethylene imine) on a reactive SAM using microcontact printing. Langmuir 15:1208–1214